Inorg. Chem. **2002**, *41*, 2282−2291

Biomimetic Studies of Terminal Oxidases: Trisimidazole Picket Metalloporphyrins

James P. Collman,* Christopher J. Sunderland, and Roman Boulatov

Department of Chemistry, Stanford University, Stanford, California 94305-5080

Received November 21, 2001

Three biomimetic models for the binuclear Fe/Cu (heme/trisimidazole) active site of terminal oxidases, such as cytochrome *c* oxidase and related enzymes, have been prepared. Based upon a tetrakis(aminophenyl)porphyrin core, these models possess a single covalently linked imidazole-bearing tail on one side of the porphyrin and three imidazole "pickets" on the opposite side of the porphyrin ring. Three different imidazole picket motifs are characterized in free base, Fe, Zn, Fe/Cu, and Zn/Cu forms. A combination of NMR, EPR, and IR demonstrates that, for the *N*-methylimidazole systems studied, the distal Cu is bound within the trisimidazole environment in the reduced (Cu(I)) and oxidized (Cu(II)) forms. The imidazole picket substitution pattern and state of metalation have significant influence on the interaction of these compounds with CO. For imidazole picket systems containing NH groups, intramolecular H bonds compete with Cu(I) coordination of the N donors.

Introduction

The consumption of oxygen in aerobic cellular respiration is primarily mediated by the multiunit enzyme cytochrome *c* oxidase (C*c*O).[1,2] This system spans the mitochondrial membrane and catalyzes the reduction of dioxygen to water while concomitantly building a transmembrane electrochemical gradient by proton translocation. The energy stored in this process is used to drive ADP phosphorylation via the similarly membrane bound, but chemiosmotically counterpoised, proton-driven ATP synthase enzyme system. Thus, dioxygen serves the dual role as terminal electron acceptor for oxidative catabolism and as energy source for the majority of ATP production. Given the advantageous energetic consequences of O_2 reduction/H^+ translocation and their efficient coupling through the C*c*O architecture, it is not surprising that considerable effort has been invested in understanding the underlying processes occurring at the molecular level. These mechanistic details involve the reaction course of small molecules interacting at the heme a_3/Cu_B site as well as the spatial and temporal issues of H^+ translocation.

A number of credible models for the heme a_3/Cu_B site have recently been synthesized[3−21] or bioengineered.[22] Particular success in structural and spectroscopic characterization has been achieved with oxidized model systems,

* To whom correspondence should be addressed. E-mail: JPC@stanford.edu.

(1) Ferguson-Miller, S.; Babcock, G. T. *Chem. Rev.* **1996**, *96*, 2889−2907.
(2) Poulos, T. L.; Li, H. Y.; Raman, C. S. *Curr. Opin. Chem. Biol.* **1999**, *3*, 131−137.
(3) Lee, S. C.; Holm, R. H. *J. Am. Chem. Soc.* **1993**, *115*, 11789−11798.
(4) Scott, M. J.; Zhang, H. H.; Lee, S. C.; Hedman, B.; Hodgson, K. O.; Holm, R. H. *J. Am. Chem. Soc.* **1995**, *117*, 568−569.
(5) Gardner, M. T.; Deinum, G.; Kim, Y.; Babcock, G. T.; Scott, M. J.; Holm, R. H. *Inorg. Chem.* **1996**, *35*, 6878−6884.
(6) Lim, B. S.; Holm, R. H. *Inorg. Chem.* **1998**, *37*, 4898−4908.
(7) Collman, J. P.; Herrmann, P. C.; Boitrel, B.; Zhang, X. M.; Eberspacher, T. A.; Fu, L.; Wang, J. L.; Rousseau, D. L.; Williams, E. R. *J. Am. Chem. Soc.* **1994**, *116*, 9783−9784.
(8) Collman, J. P.; Fu, L.; Herrmann, P. C.; Zhang, X. M. *Science (Washington, D.C.)* **1997**, *275*, 949−951.
(9) Collman, J. P.; Schwenninger, R.; Rapta, M.; Broring, M.; Fu, L. *Chem. Commun.* **1999**, 137−138.
(10) Collman, J. P.; Fu, L.; Herrmann, P. C.; Wang, Z.; Rapta, M.; Broring, M.; Schwenninger, R.; Boitrel, B. *Angew. Chem., Int. Ed.* **1998**, *37*, 3397−3400.
(11) Collman, J. P.; Rapta, M.; Broring, M.; Raptova, L.; Schwenninger, R.; Boitrel, B.; Fu, L.; M, L. H. *J. Am. Chem. Soc.* **1999**, *121*, 1387−1388.
(12) Karlin, K. D.; Nanthakumar, A.; Fox, S.; Murthy, N. N.; Ravi, N.; Huynh, B. H.; Orosz, R. D.; Day, E. P. *J. Am. Chem. Soc.* **1994**, *116*, 6, 4753−4763.
(13) Fox, S.; Nanthakumar, A.; Wikstrom, M.; Karlin, K. D.; Blackburn, N. J. *J. Am. Chem. Soc.* **1996**, *118*, 24−34.
(14) Corsi, D. M.; Murthy, N. N.; Young, V. G.; Karlin, K. D. *Inorg. Chem.* **1999**, *38*, 848−858.
(15) Kopf, M. A.; Karlin, K. D. *Inorg. Chem.* **1999**, *38*, 4922−4923.
(16) Ghiladi, R. A.; Ju, T. D.; Lee, D. H.; Moënne-Loccoz, P.; Kaderli, S.; Neuhold, Y. M.; Zuberbühler, A. D.; Woods, A. S.; Cotter, R. J.; Karlin, K. D. *J. Am. Chem. Soc.* **1999**, *121*, 9885−9886.
(17) Ghiladi, R. A.; Hatwell, K. R.; Karlin, K. D.; Huang, H. W.; Moënne-Loccoz, P.; Krebs, C.; Huynh, B. H.; Marzilli, L. A.; Cotter, R. J.; Kaderli, S.; Zuberbühler, A. D. *J. Am. Chem. Soc.* **2001**, *123*, 6183−6184.
(18) Sasaki, T.; Nakamura, N.; Naruta, Y. *Chem. Lett.* **1998**, 351−352.

10.1021/ic011191p CCC: $22.00
Published on Web 03/26/2002

Scheme 1

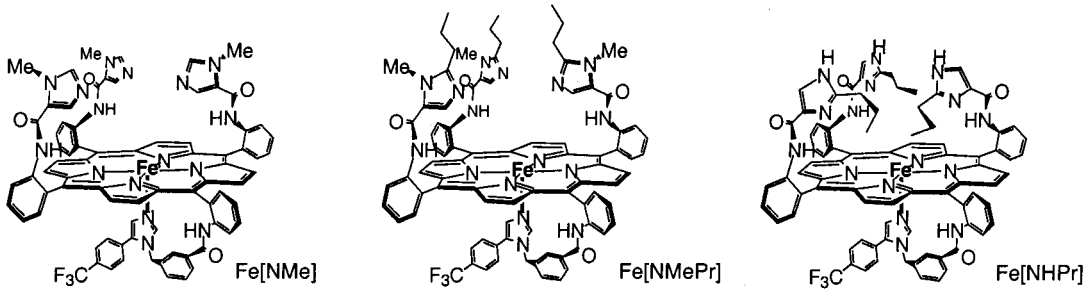

primarily as μ-oxo/hydroxo[3,4,12,13,23] or μ-cyano[5,6,14,24,25] heme−copper systems. It is also important to understand the interaction of (P)Fe/Cu(N) bimetallic complexes with other small molecules such as CO. Carbon monoxide is not only a biologically occurring inhibitor, but also a frequently employed biochemical probe for the study of C*c*O and other hemes.

In this paper, we describe the synthesis and characterization of a new family of cytochrome *c* oxidase models (Scheme 1). These compounds are the closest models to the C*c*O active site yet described. The systems consist of a trisimidazole coordination site held ∼5 Å from the porphyrin plane and a covalently attached proximal imidazole tail. The ligand design allows for the exploration of steric and H-bonding effects in the solution chemistry of such systems. In addition, the inclusion of a ^{19}F NMR tag provides a valuable analytical tool for these studies. A wealth of information has been reported for mononuclear hemes exploring steric and polarity effects around a (P)FeCO unit.[26−33] We have chosen to focus on the use of carbon monoxide adducts of our systems to afford derivatives that are stable, representative adducts of the fully reduced Fe/Cu bimetallic system. Carbon monoxide adducts of C*c*O are an essential element of O_2 kinetic studies using flash photolysis and for understanding redox interactions and proton pumping within the enzyme system.[1,34−38] Due to the structural characteristics of our catalysts, we simultaneously have access to the poorly explored chemistry of binuclear heme−copper CO adducts and a method for readily producing low-spin ($S = 0$) iron(II) porphyrin complexes to facilitate NMR analysis.

Results

Preparation of the Compounds.

The series of compounds described are denoted as α_3-ImβF$_3$T porphyrins, referring to three distal (α_3) imidazole (Im) pickets and a proximal (β) *p*-(trifluoromethyl)phenyl (F$_3$) substituted imidazole tail (T). Since the proximal tail and stereochemistry are constant, the systems are abbreviated down to the type of α_3Im cap looking at the *N*-Im and 2-Im substituents—NMe, NMePr, or NHPr (Scheme 1). The synthesis of free bases H_2[NMe], H_2[NMePr], and H_2[NHPr] was achieved using a combination of reported[39,40] and new methodologies (Scheme 2). A new synthetic refinement concerns the use of acetonitrile as solvent in the amide coupling reactions that bring the proximal and distal imidazole units together with the $\alpha_3\beta$-tetraaminoporphyrin synthon. This change decreases the excess equivalents of imidazole acid chloride required and simplifies assembly of the reaction, while providing products in higher yield and purity. For example, coupling the appropriate imidazole acid chloride (5 equiv) to the α_3AβF$_3$T provides the free bases H_2[NMe] and H_2[NMePr] in 80−90% yield. Previously,[39] H_2[NHPr] was prepared in 63% yield by using 2-propylimidazole acid chloride (9 equiv) in a sodium acetate/acetic acid system.

Metalation of the porphyrin free bases was performed in acetic acid with an excess (∼2.5 equiv) of $FeBr_2$ with lutidine as base. Acetic acid is a solvent in which the iron salt and porphyrin are readily soluble while providing a protic medium to aid displacement of iron from the imidazole pickets. Recovery of the metalloporphyrins in high purity required slightly differing conditions for each system. For Fe[NMe] and Fe[NHPr], dilution of the acetic acid solution with dichloromethane was followed by aqueous extraction, whereas Fe[NMePr] was best purified by dilution of the

(19) Naruta, Y.; Sasaki, T.; Tani, F.; Tachi, Y.; Kawato, N.; Nakamura, N. *J. Inorg. Biochem.* **2001**, *83*, 239−246.
(20) Ricard, D.; Andrioletti, B.; L'Her, M.; Boitrel, B. *Chem. Commun.* **1999**, 1523−1524.
(21) Thrash, T. P.; Wilson, L. J. *Inorg. Chem.* **2001**, *40*, 4556−4562.
(22) Sigman, J. A.; Kwok, B. C.; Lu, Y. *J. Am. Chem. Soc.* **2000**, *122*, 8192−8196.
(23) Nanthakumar, A.; Fox, S.; Murthy, N. N.; Karlin, K. D. *J. Am. Chem. Soc.* **1997**, *119*, 3898−3906.
(24) Scott, M. J.; Lee, S. C.; Holm, R. H. *Inorg. Chem.* **1994**, *33*, 4651−4662.
(25) Scott, M. J.; Holm, R. H. *J. Am. Chem. Soc.* **1994**, *116*, 11357−11367.
(26) Ray, G. B.; Li, X. Y.; Ibers, J. A.; Sessler, J. L.; Spiro, T. G. *J. Am. Chem. Soc.* **1994**, *116*, 162−176.
(27) Vogel, K. M.; Kozlowski, P. M.; Zgierski, M. Z.; Spiro, T. G. *Inorg. Chim. Acta* **2000**, *297*, 11−17.
(28) Park, K. D.; Guo, K.; Adebodun, F.; Chiu, M. L.; Sligar, S. G.; Oldfield, E. *Biochemistry* **1991**, *30*, 2333−2347.
(29) Slebodnick, C.; Duval, M. L.; Ibers, J. A. *Inorg. Chem.* **1996**, *35*, 3607−3613.
(30) Spiro, T. G.; Kozlowski, P. M. *Acc. Chem. Res.* **2001**, *34*, 137−144.
(31) Kalodimos, C. G.; Gerothanassis, I. P.; Pierattelli, R.; Troganis, A. *J. Inorg. Biochem.* **2000**, *79*, 371−380.
(32) Tetreau, C.; Lavalette, D.; Momenteau, M.; Fischer, J.; Weiss, R. *J. Am. Chem. Soc.* **1994**, *116*, 11840−11848.
(33) Collman, J. P.; Fu, L. *Acc. Chem. Res.* **1999**, *32*, 455−463.
(34) Malmstrom, B. G. *Chem. Rev.* **1990**, *90*, 1247−1260.
(35) Michel, H.; Behr, J.; Harrenga, A.; Kannt, A. *Annu. Rev. Biophys. Biomol. Struct.* **1998**, *27*, 329−356.
(36) Michel, H. *Biochemistry* **1999**, *38*, 15129−15140.
(37) Babcock, G. T. *Proc. Natl. Acad. Sci. U.S.A.* **1999**, *96*, 12971−12973.
(38) Kitagawa, T. *J. Inorg. Biochem.* **2000**, *82*, 9−18.
(39) Collman, J. P.; Broring, M.; Fu, L.; Rapta, M.; Schwenninger, R. *J. Org. Chem.* **1998**, *63*, 8084−8085.
(40) Collman, J. P.; Broring, M.; Fu, L.; Rapta, M.; Schwenninger, R.; Straumanis, A. *J. Org. Chem.* **1998**, *63*, 8082−8083.

Scheme 2

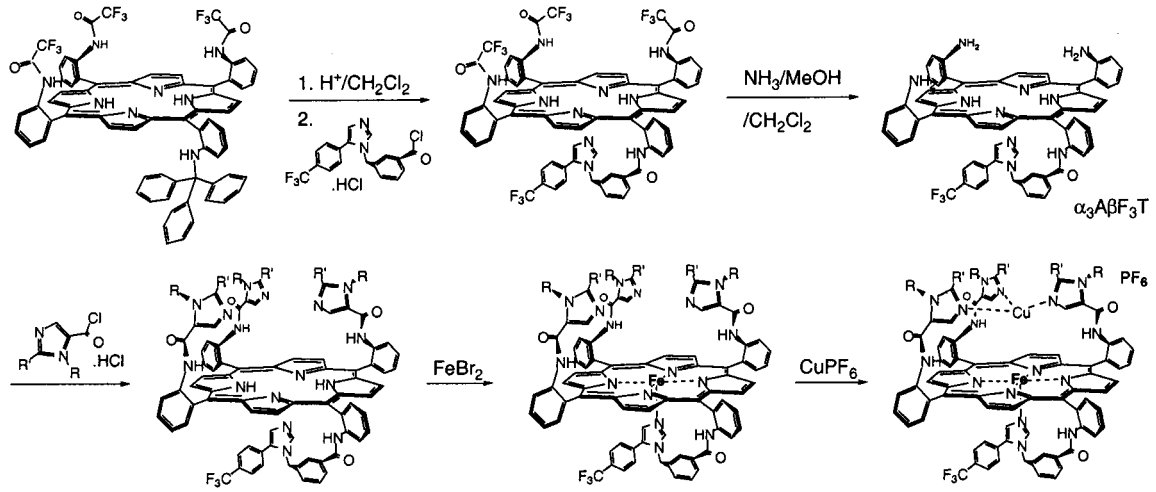

reaction with benzene. For the purification of Fe[NMe], extraction of all excess Fe(II) from the reaction required use of an aqueous Na_2EDTA solution. In the case of Fe[NHPr], due to the limiting solubility characteristics of the NH imidazole system, 10−20% 2-propanol was required to maintain solution in the organic phase as the extraction of excess Fe(II) proceeded. The greater solubility of the NMe and NMePr systems also allows for insertion of Fe(II) in a less polar solvent system of 1:4 methanol/THF at reflux. Following extractive procedures similar to those outlined above leads to the isolation of products spectroscopically indistinguishable from those obtained from the acetic acid system. Metalation of the free base porphyrins with zinc proceeded using commonly employed conditions of zinc acetate in methanol. However, as observed with the Fe insertion, EDTA was required in the extractive workup to completely demetalate the imidazole pickets of the [NMe] ligand. Since an EDTA extraction is only an obligate practice for removal of iron or zinc from the imidazole pickets of the [NMe] system, this implies it forms stronger imidazole−metal ion complexes than the 2-Pr-substituted imidazole pickets. This may be due to the lesser steric hindrance of 2-H imidazoles compared to 2-alkyl-substituted imidazole pickets. Metalation of the imidazole pickets of the metalloporphyrin with Cu[PF_6]−tetrakisacetonitrile complex was achieved by addition of 1 equiv of the Cu(I) salt to the Fe(II) complexes, typically in THF/acetonitrile mixtures.

Nuclear Magnetic Resonance Spectroscopy. For all compounds reported, full assignment of the ^{1}H NMR spectra was achieved by a combination of standard H−H COSY and NOE experiments, supplemented where necessary by comparison to precursor compounds. Full assignments are available as Supporting Information. A numbering scheme denoting the important residues discussed below is presented in Scheme 3, and some distal imidazole chemical shifts are given in Table 1. The NMe complexes could be dissolved and characterized in a number of solvents. By comparison, due to stability and solubility considerations in solvents that provided well-resolved NMR spectra across the series of free base and mono- and bimetallic [NHPr] compounds, DMF-d_7 proved to be the solvent of choice for the NH imidazole containing compounds.

Scheme 3

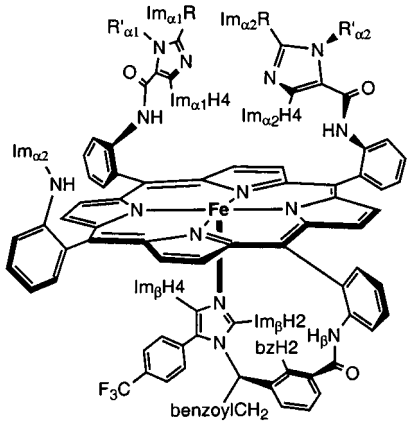

Table 1. ^{1}H NMR Chemical Shifts for Protons of the Imidazole Systems Described

system	derivative	ImH4[a]	Im2-sub[b]
[NMe][c]	H_2	5.39	6.94
	Fe	5.30	6.89
	Zn	5.12	6.80
	Fe/Cu	5.14	7.33
	Zn/Cu	4.72	6.96
PhNMe[c]		7.53	7.60
[NMePr][c]	H_2	5.25	1.51
	Fe	5.00	1.48
	Zn	4.93	1.43
	Fe/Cu	4.87	1.58
	Zn/Cu	4.05	1.51
[NHPr][d]	H_2	7.28	0.05
	Fe	7.38	0.49
PhNHPr[d]		7.78	1.71

[a] Weight average of the α1 and α2 ImH4 chemical shifts. [b] For 2-Pr-substituted systems, the value is the weight average δ of all protons of the α1 and α2 Pr groups; for [NMe], the value is the weight average of the α1 and α2 ImH2 chemical shifts. [c] Solvent for free base and monometallic systems, $CDCl_3$; for bimetallic systems, 10% ACN-d_3/THF-d_8. [d] In DMF-d_7.

The NMR spectra of H_2[NMe] and H_2[NMePr] demonstrate some atypical chemical shifts for the picket imidazole resonances compared to those of non-porphyrin analogues such as the aniline amides of the corresponding 4-imida-

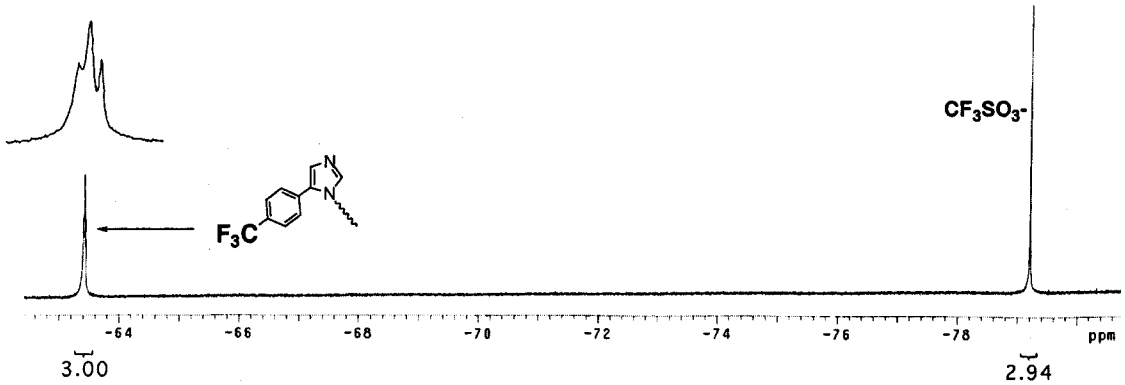

Figure 1. ^{19}F NMR spectrum of {Fe/Cu[NHPr]·CO}OTf in DMF-d_7 demonstrating the presence of at least three product isomers.

zolecarboxylic acids (abbreviated PhNMeIm and PhNMePrIm, respectively). The chemical shift of the diagnostic α-ImH4 resonances (δ_{H4}{H_2[NMe]} 5.4; δ_{H4}{H_2[NMePr]} 5.2) is strongly shifted upfield from its position observed in H_2[NHPr] (δ_{H4} 7.3) and from the position of this resonance in the simple aniline amide of this imidazole (PhNMeIm, δ_{H4} 7.5) (Table 1). Proton resonances at the 2-Im position convey the opposite trends. For both [NMe] and [NMePr] the weight-averaged chemical shift of the 2-Im substituent (H or Pr) is within 0.3−0.8 ppm of that of the corresponding non-porphyrin analogue. This suggests that the resonances of the α-ImH4 protons but not those of the 2-substituent are most significantly shifted by the porphyrin ring current.

The NMR spectra of Fe[NMe]·CO and Fe[NMePr]·CO indicate that the distal imidazole picket structures are similar to the picket structure of H_2[NMe] and H_2[NMePr]; the resonances of the key protons mentioned above undergo only small chemical shift changes compared to those of the free base. In contrast to those of the α-Im pickets, the resonances of the proximal tail assembly (especially those of the ImβH2/H4 protons) undergo dramatic upfield shifts compared to those of the free bases as the tail imidazole coordinates the iron center, bringing protons of both the proximal base and the linker in close proximity to the porphyrin ring. A series of NOE enhancements linking the proximal amide NH to the CF_3Ph CH's clearly identifies these spatially close protons, providing confirmation of the assignments made from structurally related compounds and H−H COSY experiments. The ^{19}F NMR spectrum consists of a singlet in each case, consistent with the presence of a single species.

Under an atmosphere of CO gas, bimetallic systems Fe/Cu[NMe] and Fe/Cu[NMePr] demonstrate NMR spectroscopic properties consistent with the formation of a single compound in solution. Neither compound shows dramatic NMR spectral changes compared to its Fe-only precursor. As in C*c*O, Cu does not prevent binding of CO to the Fe center due to the 4−5 Å separation of these metals. Formation of a complex with 1 equiv of Cu was checked by integration of the CF_3 signal of the porphyrin tail to the Cu(I) counterion ($CF_3SO_3^-$ or PF_6^-). All Fe/Cu systems used in the spectroscopic and chemical studies met this criterion of 1:1 stoichiometry. Furthermore, the molecular weights of all reported free base and mono- and bimetallic compounds were confirmed by mass spectrometry.

Notably, the resonances of the imidazole 2-Pr groups of H_2[NHPr] are shifted upfield by a weight average of 1.7 ppm compared to those of its corresponding non-porphyrin analogue, PhNHPrIm. By contrast, the resonances of the α-ImH4 protons of H_2[NHPr] are shifted upfield by less than 0.5 ppm relative to that of the ImH4 proton in PhNHPrIm. Thus, in contrast to the NMe systems, it is the resonances of the 2-Pr, not α-ImH4, protons that are most significantly shifted by the porphyrin ring current. As observed in NMe systems, the distal pickets of the metalated derivative Fe[NHPr]·CO possess NMR characteristics similar to those of the corresponding free base forms. The proton resonances of the imidazole tail structure shift upfield, indicating that the covalently linked imidazole tail coordinates the iron.

All the [NMe], [NMePr], H_2[NHPr], and Fe[NHPr] complexes demonstrate NMR characteristics consonant with single compounds of the symmetry expected. By contrast, Fe/Cu[NHPr] demonstrates a complex NMR spectrum, indicating formation of more than one type of Cu(I) coordination complex. This mixture could not be driven to a single isomer by a change of temperature, solvent, Cu(I) counterion, or reaction time. Under an atmosphere of CO, at least three compounds are apparent in the ^{1}H NMR. The ^{19}F NMR confirms the presence of at least three compounds (Figure 1). Since the addition of Cu(I) to Fe[NHPr] does not result in the formation of a discrete entity, analysis of the Fe/Cu[NHPr] solution conformation is more difficult.

Optical Spectroscopy. The visible absorption spectra of the Fe and Fe/Cu complexes of [NMe], [NMePr], and [NHPr] demonstrate Soret bands in the region of 422−428 nm, which is consistent[41] with a 6-coordinate, reduced (Fe(II) or Fe(II)/Cu(I)) system. The single exception is Fe[NMePr], which possesses a Soret band at 438 nm, typical for a 5-coordinate heme.[41] Since the Fe-only systems are prepared with aqueous extractions, and no evidence for 1 equiv of another solvent is found in the NMR spectra of these materials under CO, the sixth coordination site is presumed to be filled by a water molecule before reaction with CO. Traces of water were frequently detected by NMR spectroscopy. Trapping of water in the distal site may be enhanced by hydrogen bonding from the imidazole N donors.

(41) Collman, J. P.; Brauman, J. I.; Doxsee, K. M.; Halbert, T. R.; Bunnenberg, E.; Linder, R. E.; Lamar, G. N.; Delgaudio, J.; Lang, G.; Spartalian, K. *J. Am. Chem. Soc.* **1980**, *102*, 4182−4192.

Table 2. Infrared Stretching Frequencies for Fe-Bound CO in Methylene Chloride

	FeC−O stretch (cm^{-1})			FeC−O stretch (cm^{-1})	
model system	no Cu(I)	with Cu(I)	model system	no Cu(I)	with Cu(I)
Fe[NMe]	1979	1950 (1954)[a]	Fe[T_{piv}PP]·NMeIm[c]	1969	
Fe[NMePr]	1978	1950[b]	Fe[TPP]·NMeIm[c]	1970	
Fe[NHPr]	1979	1961[b]	cytochrome *bo* H333A[d]	1970	1960
Fe[α_3AcβF$_3$T]	1968		C*c*O H333L[e]	1971	1959

[a] 1950 value measured under trace CO atmosphere, 1954 value measured under 1 atm of CO. [b] CO stretching frequency invariant with CO partial pressure. [c] In benzene solution.[49] [d] No Cu is the H333A mutant; with Cu is the wild type.[50] [e] No Cu is the H333L mutant; with Cu is the wild type.[51]

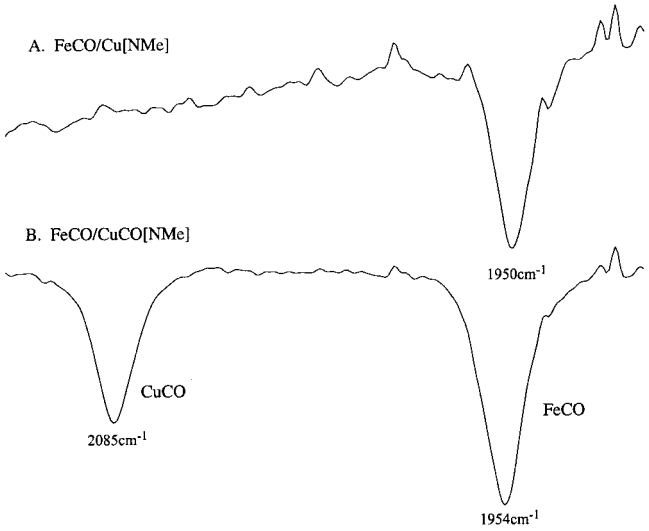

Figure 2. Infrared spectra of Fe/Cu[NMe] under trace CO (A) and under an atmosphere of CO (B).

Table 3. Infrared Stretching Frequencies for CO Bound in the Distal $Cu(Im)_3$ Chelate

	CuC−O stretch (cm^{-1})		CuC−O stretch (cm^{-1})
Fe/Cu[NMe]	2085	Zn/Cu[NMe]	2087
Fe/Cu[NMePr]	−	Zn/Cu[NMePr]	2079

Infrared Spectroscopy. In dichloromethane solutions of ~1.5 mM concentration, all three iron(II) porphyrins bind CO and demonstrate a CO stretching frequency of ~1979 cm^{-1}, as expected for the (P)FeCO stretch. The bimetallic Fe/Cu systems of [NMe] and [NMePr] demonstrate ν(CO) of 1950 and 1954 cm^{-1}, respectively, under trace CO (Table 2). Under an atmosphere of CO, Fe/Cu[NMe] also demonstrates an absorption at 2085 cm^{-1}, which is assigned as the CuCO stretch (Figure 2). By comparison, Zn/Cu[NMe] and Zn/Cu[NMePr] demonstrate CO stretching frequencies of 2087 and 2079 cm^{-1}, respectively, under an atmosphere of CO (Table 3).

EPR Spectroscopy. The Zn/Cu(II)[NMe] complex is useful for defining, by EPR spectroscopy, the coordination geometry at Cu(II) resulting from this particular trisimidazole ligand (Figure 3). Typical for frozen-solution EPR spectra of Cu(II) species, the Zn/Cu(II) complex exhibits an axial **g** tensor, since small anisotropies in the equatorial plane are obscured by relatively large widths of the parallel absorption peaks. Spin Hamiltonian parameters, obtained by simulating the experimental spectrum,[42] agree well with the literature

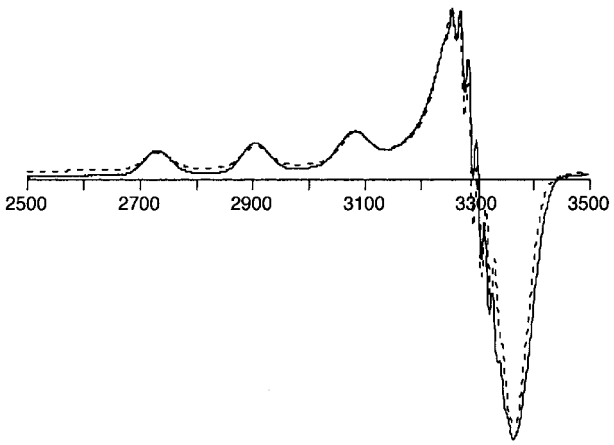

Figure 3. EPR spectrum of Zn/Cu[NMe]Cl(PF_6) at 77 K in DMF, measured (solid line) and simulated (dashed line). $g_{||} = 2.28$, $g_{\perp} = 2.07$, $A_{||} = 175$ G, $A_{\perp} = 13$ G, and $A_{||}(^{14}N) = 15$ G.

data for Cu(II) centers coordinated to nitrogenous ligands.[43−45] The resolved pattern of the ^{14}N-superhyperfine coupling is restricted to the perpendicular region, which precludes straightforward determination of the number of N atoms bound to the Cu. A possibility that the EPR spectrum arises from Cu coordinated to only two N atoms can be excluded, since the experimental spectrum could not be simulated satisfactorily with a CuN_2 core. Adequate agreement between the simulated and the experimental EPR spectra was obtained for the CuN_3 and CuN_4 cores. However, the CuN_4 geometry requires that more than one porphyrin moiety is associated with a single Cu^{2+} ion. A combination of two pieces of data—the overall 1:1 Zn[NMe]:Cu(II) stoichiometry of the sample, and the presence of a single species suggested by the ^{19}F NMR and EPR spectroscopies—excludes such aggregates as the dominant species in solution or in the frozen glass. The relatively large value of $A_{||}$ (175 G) is consistent with an essentially square-planar geometry around the Cu^{2+}.[46]

Discussion

The fully reduced forms of our C*c*O models present experimental challenges due to air sensitivity. This is especially apparent for the bimetallic Fe/Cu systems. However, isolation and purification of these reduced species provide a bulk supply of the catalytically active (oxygen-

(42) *Win-EPR SimFonia v1.25*; Bruker Analytische: Karlsruhe, Germany, 1996.

(43) Bonomo, R. P.; Riggi, F.; Dibilio, A. J. *Inorg. Chem.* **1988**, *27*, 2510−2512.
(44) Siddiqui, S.; Shepherd, R. E. *Inorg. Chem.* **1986**, *25*, 3869−3876.
(45) Santagostini, L.; Gullotti, M.; Pagliarin, R.; Bianchi, E.; Casella, L.; Monzani, E. *Tetrahedron: Asymmetry* **1999**, *10*, 281−295.
(46) Hathaway, B. J. *Comprehensive Coordination Chemistry*; Pergamon Press: New York, 1987; Vol. 5, p 153.

Scheme 4

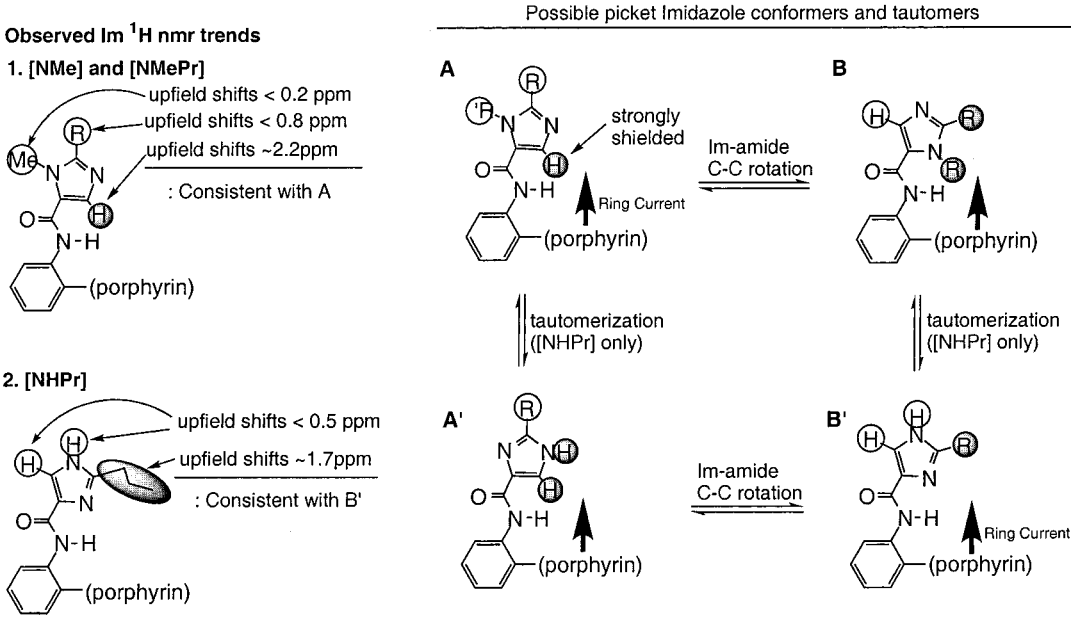

binding) form of these molecules. Additionally, iron(II) porphyrins react with CO to form low-spin ($S = 0$) complexes, affording an excellent opportunity to compare the solution behavior of the free base, Fe, and Fe/Cu systems within the normal diamagnetic NMR spectral envelope. The infrared characteristics of such carbonyls are also well documented due to the biological relevance of carbon monoxide inhibited hemes.

Since the ligand design for this family of C*c*O models uses amide linkages to position the Cu binding locus within ~4−5 Å of the iron center, the resultant imidazole pickets have limited conformational freedom and are in close proximity to the porphyrin plane. Due to the large ring current effect of porphyrins, the chemical shifts of protons in appended groups provide information about the picket orientation relative to the porphyrin ring.[47] Indeed, inspection of the NMR spectra of [NHPr] compounds compared to the NMe models demonstrates solution structure characteristics important to the application of NH systems as a whole.

The picket imidazoles can be represented in four distinct ways composed of differing conformational and tautomeric structures (Scheme 4). A strong downfield shift of the α-ImH4 protons, but not of the 2-Im substituent protons, of both NMe compounds is observed. This indicates that the ImH4 groups are close to the shielding influence of the porphyrin ring such as in conformations A and B. Conformation B is not expected to significantly contribute to the solution structure on the basis of steric (porphyrin ring/NMe) arguments alone. Given the alkylation on N1, these shifts uniquely implicate structure A (Scheme 4) as the geometry most representative of the distal picket conformation in these N-methylated derivatives. Thus, the trisimidazole picket motif of the NMe compounds can be considered predisposed toward metal ion complexation above the Fe center. This conclusion is supported by the observation that the corresponding Cu(I) complexes demonstrate an NMR spectrum consistent with the formation of a single compound of the correct symmetry, and with few chemical shift changes from that of the Fe-only complexes. Changes in the NMR spectrum of FeCO/Cu[NMe] in the absence and presence of a CO head gas (Figure 4) implicate CO binding to Cu. Further analysis by IR spectroscopy (see below) strengthens these arguments and supports the ligand geometry depicted in Scheme 1 as being representative of the extant solution structure for H_2[NMe], Fe[NMe], Fe/Cu[NMe], H_2[NMePr], Fe[NMe], and Fe/Cu[NMePr].

It is readily apparent from NMR spectroscopy that the distal picket structures of the [NHPr] compounds are at variance to those deduced for the [NMe] and [NMePr] lineage. A strong downfield shift of the protons of the 2-Pr groups, but not of the H4 imidazole proton, of H_2[NHPr] indicates that the propyl groups are close to the shielding influence of the porphyrin ring such as in conformations B and B′. Structure B is expected to possess unfavorable steric and dipole amide NH/ImNH interactions, whereas conformation B′ includes a strong amide NH···NIm hydrogen bond. This analysis suggests that the distal cap environment of H_2-[NHPr] is best described by structure B′ (Scheme 4) rather than an alternate tautomer such as B or other structures such as A or A′. Therefore, it is concluded that the amide NH−imidazole N1 hydrogen bond is the dominant structural influence in the cap system and effectively competes against the alternative H-bonding opportunity between the imidazole NH and amide oxygen donor−acceptor pair apparent in structure A. Crystallographic evidence confirming the presence of this internal amide NH−imidazole N1 H bond has been observed in a related α_4-imidazole-picketed porphyrin.[48] This distal site structure is believed to persist in the Fe[NHPr]

(47) Wuenschell, G. E.; Tetreau, C.; Lavalette, D.; Reed, C. A. *J. Am. Chem. Soc.* **1992**, *114*, 3346−3355.

(48) Collman, J. P.; Berg, K. E.; Aukauloo, A.; Sunderland, C. J. To be published.

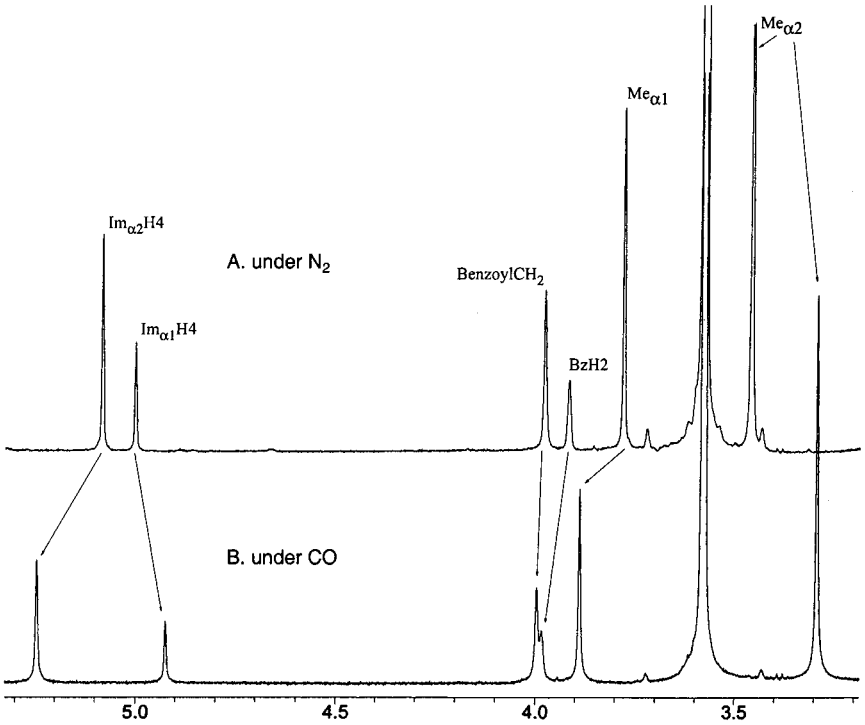

Figure 4. Changes in the ^{1}H NMR spectrum of selected resonances in FeCO/Cu[NMe]·PF_6 upon exchange of a dinitrogen atmosphere (A) for a CO atmosphere (B) to give FeCO/CuCO[NMe]·PF_6 in 10% ACN-d_3/THF-d_8.

system as similar trends in the shifts of the imidazole 2-Pr and H4 protons exist. An important consequence of this strong internal H-bonding is the resultant competition for the imidazole N3 donor, which is required for coordination of Cu in the desired (P)Fe/Cu(Im)$_3$ bimetallic system. The mixture of coordination compounds observed in the Fe/Cu-[NHPr] system, which is apparent by ^{1}H and ^{19}F NMR spectroscopy, is believed to originate from the strong internal H bonds, which lead to a mixture of Cu(Im)$_x$(solv)$_y$ structures. The histidine residues chelating Cu in the active site of C*c*O possess NH groups which are speculated to be crucial to the catalytic activity of the enzyme. These ImNH-containing models are desirable from the perspective of investigating the influence of H bond donation on catalytic activity. However, the problems found in obtaining discrete coordination compounds with weakly binding metal ions indicates that such investigations will be difficult at the basic level of characterization.

Infrared spectra of the Fe and Fe/Cu carbon monoxide adducts of [NMe], [NMePr], and [NHPr] provide significant information regarding the solution characteristics of the reduced forms of our catalyst systems. The IR spectra of all three Fe[α_3ImβF$_3$T]·CO systems are essentially the same: Fe[NMe] (1979 cm^{-1}), Fe[NMePr] (1978 cm^{-1}), Fe[NHPr] (1979 cm^{-1}). This frequency is higher than normally demonstrated by such model compounds (Table 1).[26,49] For comparison, a related compound, Fe[α_3AcβF$_3$T], was prepared where the imidazole pickets are replaced by acetyl amides, while retaining the same proximal structure. FeCO-[α_3AcβF$_3$T] has a carbonyl stretching frequency of 1968 cm^{-1}, typical of simple (P)FeCO complexes with an imidazole axial base. Therefore, structural or electronic influences from the tethered proximal imidazole can be excluded as a reason for the high CO stretching frequency found in the imidazole-appended systems. The correlation between (P)-FeCO structures and CO stretching frequencies has been investigated for a number of heme proteins and superstructured models. In general, when the axial ligand is invariant, electrostatic interactions within the distal site where CO binds primarily influence the CO stretching frequency of (P)FeCO adducts.[26−31] Specifically, elevated CO stretching frequencies are typically associated with electrostatic interactions of the CO with negative dipoles such as those of aromatic rings or lone pairs. The high CO stretching frequency of the FeCO-[α_3ImβF$_3$T] systems compared to the FeCO[α_3AcβF$_3$T] adduct is consistent with the presence of the imidazole donor groups positioned above the heme. The lone pairs of the imidazoles are expected to electrostatically destabilize CO back-bonding, leading to an increase in the CO stretching frequency relative to those of Fe[α_3AcβF$_3$T] and similarly picketed porphyrins.

The CO stretching frequencies of the Fe/Cu complexes are quite different from those of the Fe-only complexes. The Fe-bound CO frequencies for FeCO/Cu[NMe] and FeCO/Cu[NMePr] are both 1950 cm^{-1} (Table 2). The decrease in CO frequency from 1978 to 1950 cm^{-1} is attributed to the positive charge of Cu(I) stabilizing back-bonding to the carbonyl, which leads to weakening of the C−O bond. The difference in the CO frequency of the Fe/Cu system compared to the Fe analogue indicates that the Cu$^+$ is in proximity of the FeCO unit; i.e., the Cu is coordinated within the pickets. This result can be directly compared to studies

(49) Collman, J. P.; Brauman, J. I.; Collins, T. J.; Iverson, B. L.; Lang, G.; Pettman, R. B.; Sessler, J. L.; Walters, M. A. *J. Am. Chem. Soc.* **1983**, *105*, 3038−3052.

on cytochrome *bo* ubiquinol oxidase.[50] As with C*c*O, this oxidase catalyzes the $4e^-$ reduction of dioxygen to water at a structurally similar (P)Fe/Cu(His)$_3$ site. Deletion of a Cu-binding imidazole group in the H333A mutant produces an enzyme that no longer binds Cu due to substitution of a Cu_B histidine ligand with a noncoordinating alanine residue. The CO frequency of the wild-type (Fe/Cu) enzyme (1960 cm^{-1}) is at higher energy in the H333A (Cu_B-free) adduct (1970 cm^{-1}). This was attributed to removal of the Cu(I) cation from the binding pocket and consequently diminished Fe−CO back-bonding.[50] Similar results have been obtained via mutagenesis in other terminal oxidase studies, with ν(FeC−O) shifts of 0−20 cm^{-1} observed in H333 mutants.[51,52] Our model systems support the argument of dipole-induced changes to the CO stretching frequency. Undoubtedly, the shift in CO stretching frequency is a product of removing the δ^- charge of the imidazole N lone pairs by complexation, while adding the δ^+ charge of Cu, perhaps with collateral steric-induced CO distortion effects.[30]

When FeCO/Cu[NMe] is prepared under an atmosphere of CO gas, an additional carbonyl stretch is observed at 2085 cm^{-1}. This is within the typical CO stretching frequency range of approximately 1950−2100cm^{-1} for CO bound to Cu(I) in a variety of N_3Cu environments.[53−61] It has been generally demonstrated that imidazoles form Im_3CuCO complexes but not Im_2CuCO complexes.[53,54,62] Furthermore, in reported (non-imidazole) N_2CuCO complexes, the CO frequency is at higher energy (2112−2117 cm^{-1}).[53,63] For the FeCO/CuCO[NMe] system, the shift of the Fe-bound CO stretch (compared to that of FeCO[NMe]) and the frequency of the CuCO stretch suggest that Cu(I) is in a trisimidazole environment over the Fe center.

It is notable that the FeCO/Cu[NMePr] system does not form a Cu−CO complex under 1 atm of carbon monoxide. The low affinity of CO toward the copper ion in FeCO/Cu[NMePr] but not in FeCO/Cu[NMe] may be attributed to steric hindrance from the propyl groups in Fe/Cu[NMePr]. This hindrance may lead to the lowered affinity of CO for the Im_3Cu chelate or lead to an Im_2Cu coordination complex which is unreactive to CO. The distal site copper−imidazole chemistry was further probed by synthesis of the zinc porphyrin analogues to these hemes. In the zinc analogues the intrinsic Im_3 coordination geometry should be identical to that found in the Fe/Cu complexes. However, CO does not bind to zinc in the porphyrin, thus leading to one less steric element centered in the picket cavity. Zn/Cu[NMe] and Zn/Cu[NMePr] demonstrate CuCO stretching frequencies of 2087 and 2079 cm^{-1}, respectively, although the relative intensity of the CuCO stretch in the [NMePr] system is attenuated. The CO stretching frequencies suggest both Zn systems are able to achieve a trisimidazole coordination at Cu(I). That the Cu of Zn/Cu[NMePr], but not FeCO/Cu[NMePr], binds CO (under 1 atm of CO gas) indicates that the propyl groups of the MePrIm pickets are not the only factor leading to the low affinity of CO for Cu in the FeCO/Cu[NMePr] system. Instead, it suggests that the additive steric effects of the 2-propyl group and FeCO unit result in disruption of CO binding to Cu. Carbon monoxide binding to the Cu site of other C*c*O models has not been previously reported, although it is a known intermediate in the formation and dissociation of the heme CO complex of C*c*O.[64−68]

EPR spectroscopy of the Zn/Cu(II)[NMe] complex demonstrates spectral parameters that are consistent with the copper ion coordinated in a square-planar environment. This coordination geometry and the singularity of composition demonstrated by ^{19}F NMR and EPR spectroscopies are consistent with the formation of a trisimidazole−Cu(II) complex. The fourth coordination site is expected to be filled by chloride, the counterion introduced during preparation. Thus, it has been demonstrated that the design of the distal imidazole superstructure allows for accommodation of the geometric requirements of both the Cu(I) and Cu(II) ions. This is important given that the Fe/Cu binuclear site must cycle between Fe(II)/Cu(I) and Fe(III)/Cu(II) during catalytic turnover of oxygen. All complexes (both monometallic and bimetallic) manifest clean 4 electron reduction of O_2 when adsorbed on an electrode in contact with aqueous buffered solution at pH 7 at moderate overpotentials, which is the subject of future publications.[69]

(50) Uno, T.; Mogi, T.; Tsubaki, M.; Nishimura, Y.; Anraku, Y. *J. Biol. Chem.* **1994**, *269*, 11912−11920.
(51) Calhoun, M. W.; Hill, J. J.; Lemieux, L. J.; Ingledew, W. J.; Alben, J. O.; Gennis, R. B. *Biochemistry* **1993**, *32*, 11524−11529.
(52) Hosler, J. P.; Kim, Y. K.; Shapleigh, J.; Gennis, R.; Alben, J.; Ferguson-Miller, S.; Babcock, G. *J. Am. Chem. Soc.* **1994**, *116*, 5515−5516.
(53) Sorrell, T. N.; Jameson, D. L. *J. Am. Chem. Soc.* **1983**, *105*, 6013−6018.
(54) Sorrell, T. N.; Borovik, A. S. *J. Am. Chem. Soc.* **1987**, *109*, 4255−4260.
(55) Karlin, K. D.; Tyeklar, Z.; Farooq, A.; Haka, M. S.; Ghosh, P.; Cruse, R. W.; Gultneh, Y.; Hayes, J. C.; Toscano, P. J.; Zubieta, J. *Inorg. Chem.* **1992**, *31*, 1436−1451.
(56) Kitajima, N.; Fujisawa, K.; Fujimoto, C.; Morooka, Y.; Hashimoto, S.; Kitagawa, T.; Toriumi, K.; Tatsumi, K.; Nakamura, A. *J. Am. Chem. Soc.* **1992**, *114*, 1277−1291.
(57) Carrier, S. M.; Ruggiero, C. E.; Houser, R. P.; Tolman, W. B. *Inorg. Chem.* **1993**, *32*, 4889−4899.
(58) Sorrell, T. N.; Allen, W. E.; White, P. S. *Inorg. Chem.* **1995**, *34*, 952−960.
(59) Mahapatra, S.; Halfen, J. A.; Wilkinson, E. C.; Pan, G. F.; Wang, X. D.; Young, V. G.; Cramer, C. J.; Que, L.; Tolman, W. B. *J. Am. Chem. Soc.* **1996**, *118*, 11555−11574.
(60) Berreau, L. M.; Halfen, J. A.; Young, V. G.; Tolman, W. B. *Inorg. Chem.* **1998**, *37*, 1091−1098.
(61) Rondelez, Y.; Seneque, O.; Rager, M. N.; Duprat, A. F.; Reinaud, O. *Chem.−Eur. J.* **2000**, *6*, 4218−4226.
(62) LeClainche, L.; Giorgi, M.; Reinaud, O. *Eur. J. Inorg. Chem.* **2000**, 1931−1933.
(63) Pasquali, M.; Floriani, C.; Gaetanimanfredotti, A. *Inorg. Chem.* **1980**, *19*, 1191−1197.
(64) Alben, J. O.; Moh, P. P.; Fiamingo, F. G.; Altschuld, R. A. *Proc. Natl. Acad. Sci. U.S.A., Biol. Sci.* **1981**, *78*, 234−237.
(65) Fiamingo, F. G.; Altschuld, R. A.; Moh, P. P.; Alben, J. O. *J. Biol. Chem.* **1982**, *257*, 1639−1650.
(66) Einarsdottir, O.; Dyer, R. B.; Lemon, D. D.; Killough, P. M.; Hubig, S. M.; Atherton, S. J.; Lopezgarriga, J. J.; Palmer, G.; Woodruff, W. H. *Biochemistry* **1993**, *32*, 12013−12024.
(67) Liebl, U.; Lipowski, G.; Negrerie, M.; Lambry, J. C.; Martin, J. L.; Vos, M. H. *Nature (London)* **1999**, *401*, 181−184.
(68) Iwase, T.; Varotsis, C.; ShinzawaItoh, K.; Yoshikawa, S.; Kitagawa, T. *J. Am. Chem. Soc.* **1999**, *121*, 1415−1416.
(69) Collman, J. P.; Boulatov, R.; Shiryaeva, I.; Sunderland, C. J. Manuscript in preparation.

Conclusions

We have developed a series of C*c*O models that demonstrate close structural analogy to the catalytic site of C*c*O. The three systems here represent a series of superstructured porphyrins that explore a variety of characteristics found to be of importance to the structure and reactivity of these imidazole picket C*c*O models. The presence of NH donors in the distal site, while desirable from the perspective of providing chemical similarity to the active site of C*c*O, presents problems to the solution characterization of the bimetallic Fe/Cu complex. *N*-Me-containing imidazoles alleviate the problems encountered with H-bonding and poor solubility, while supporting an imidazole donor orientation predisposed toward metal ion complexation. Unique to the many reported C*c*O models, we have been able to demonstrate that Cu(I) binding affects the frequency of the heme FeC−O stretch, and that CO binding to the Cu is moderated by steric effects of both imidazole substitution and the presence of a sixth axial ligand on the porphyrin-based metal. The distal copper has been shown to reside within the trisimidazole picket coordination environment, in both Cu(I) and Cu(II) forms of the system.

Experimental Section

Materials. Reagents and solvents were of commercial reagent quality unless otherwise noted. Under an inert atmosphere, tetrahydrofuran, benzene, toluene, and diethyl ether were distilled from sodium benzophenone ketyl while acetonitrile and dichloromethane were distilled from CaH_2 prior to use. For NMR studies, THF-d_8 was vacuum transferred from sodium benzophenone ketyl and $CDCl_3$ and CD_2Cl_2 were vacuum transferred from 4 Å molecular sieves into flame-dried NMR tubes immediately prior to use. MeCN-d_3 and DMF-d_7 were degassed (three freeze−pump−thaw cycles), transferred to a glovebox, and stored over 4 Å molecular sieves in vials closed with septa. AcOD-d_3 was stored over 4 Å molecular sieves. 1-Methylimidazole-5-carboxylic acids and their corresponding acid chlorides were prepared by previously described methods[39,70] as modified below. The precursor common to the α_3-ImβF$_3$T systems, α,α,α-tris(*o*-aminophenyl)-β-(*o*-3-(1-(5-*p*-trifluoromethylphenyl)imidazolylmethyl)benzamidophenyl)porphyrin (α_3AβF$_3$T),[40] and H_2[NHPr] were prepared as reported.[39]

Methods. Chromatography was performed under reduced lighting to retard decomposition of the superstructured porphyrin systems on silica adsorbants. Synthesis of air-sensitive porphyrin compounds was performed in a Vacuum Atmospheres glovebox under a N_2 atmosphere with <1 ppm O_2 content. All porphyrin and metalloporphyrin NMR samples were prepared under an inert (N_2) atmosphere in 5 mm NMR tubes fitted with PTFE valves. Metalloporphyrin carbonyl adduct NMR samples were formed by freezing the NMR tube solution in liquid N_2, removing the volatile inert head gas, and backfilling the tube with CO to provide approximately 1 atm of CO above the sample. UV/vis samples were prepared in a glovebox. IR samples were prepared by injecting solutions of metalloporphyrin into a carbon monoxide flushed IR cell.

Instrumentation. All NMR spectra were recorded on a Varian Unity 500 spectrometer. ^{1}H NMR spectra were referenced to the residual protio solvent signal. ^{19}F NMR spectra were referenced to $CFCl_3$ (0 ppm). UV/vis spectra were recorded on an HP8452A spectrometer at a concentration of $\sim 2 \times 10^{-5}$ to 10^{-6} M. IR spectra were recorded on a Mattheson Infinity Series FTIR spectrometer in a NaCl solution cell (path length 1.0 mm) with concentrations of ~1.5 mM. EPR spectra were recorded on a Brucker ER 220D-SRC spectrometer at 77 K in a 3 mm (o.d.) quartz tube fitted with a PTFE valve on a 2 mM solution of the analyte in DMF glassified by rapid freezing with liquid N_2.

General Procedures. Synthesis of 5-Imidazole Acid Chloride Hydrochlorides. The appropriate 5-imidazolecarboxylic acid hydrochloride (6.77 mmol)[39,70] was stirred as a suspension in dry acetonitrile (30 mL). Oxalyl chloride (1.0 mL, 11 mmol) was added over 10−15 s followed by one drop of DMF. After 4 h the straw-colored solution was reduced in volume to 8−10 mL under dynamic vacuum without external heating. The chill suspension was filtered and the residue washed with acetonitrile until the washings were colorless. Drying under high vacuum afforded the product as a dense white crystalline solid (85−98%).

Data for NMeImCl·HCl. ^{1}H NMR (AcOD-d_3): δ 9.41 (s, 1H, Im-2-H), 8.55 (s, 1H, Im-4-H), 4.13 (s, 3H, NMe).

Data for NMe-2-PrImCl·HCl. ^{1}H NMR (AcOD-d_3): δ 8.16 (s, 1H, Im-4-H), 4.05 (s, 3H, NMe), 3.13 (t, J = 7.7 Hz, 2H, Im-2-CH_2CH$_2$CH$_3$), 1.88 (sextet, J = 7.3 Hz, 2H, Im-2-CH$_2$CH_2CH$_3$), 1.04 (t, J = 7.3 Hz, 3H, Im-2-CH$_2$CH$_2$CH_3).

Synthesis of Free Base Porphyrins H_2[NMe] and H_2[MePr]. To the appropriate imidazole acid chloride (450 μmol) in dry acetonitrile (25 mL) were added α_3AβF$_3$T (90 μmol) and diisopropylethylamine (270 μmol) over 90 min (for the H_2[NMe] system) or 40 min (for H_2[NMePr]), followed by stirring for 10 min. Trace amounts of mono- and bisimidazole-substituted porphyrins will remain. The solution was evaporated to approximately 5 mL, diluted with CH_2Cl_2 (50 mL), and washed with 50% saturated $NaHCO_3$ (50 mL) and then water (50 mL). After drying (Na_2CO_3) and chromatography (silica gel, 2−5% MeOH in CH_2Cl_2 (50% saturated in NH_3 gas)), an 80−90% yield of H_2[α_3ImβF$_3$T] porphyrin was obtained.

Data for H_2[NMe]. MS (ES): *m*/*e* 1327.5 [MH]$^+$, calcd for [MH]$^+$ 1327.4. NMR assignments are given in the Supporting Information.

Data for H_2[NMePr]. MS (ES): *m*/*e* 1453.7 [MH]$^+$, calcd for [MH]$^+$ 1453.6. NMR assignments are given in the Supporting Information.

Synthesis of Iron(II) Porphyrins. Method A. To a solution of the free base porphyrin (~100 μmol) in acetic acid (20 mL) were added $FeBr_2$ (2.5 equiv) and lutidine (10 drops). The mixture was stirred overnight (or for at least 5 h) and then diluted with 20 mL of solvent (for [NHPr], 10% 2-propanol/CH_2Cl_2; for [NMe], CH_2Cl_2; for [NMePr], benzene). The organic phase was washed with water (20 mL), Na_2EDTA (20 equiv in 20 mL of water), and water again (20 mL) followed by drying (Na_2SO_4) and evaporation of the solvent. The residue was redissolved in THF (10 mL) with MeOH added dropwise if solution was not achieved in 30 min. Toluene (10 mL) was then added, and the solvents were removed under high vacuum. The product was redissolved in benzene (10 mL) and a few drops of methanol added to complete dissolution if necessary. After freeze-drying under high vacuum, the iron(II) porphyrins were obtained in 85−95% yield.

Method B. To a solution of free base porphyrin (H_2[NMe] or H_2[NMePr]) (~20 μmol) in 20% MeOH/THF (20 mL) at reflux was added $FeBr_2$ (2.5 equiv), and heating was continued for 45 min. The volume was reduced to ~5 mL and the solution diluted with 0.1 M aqueous ETDA solution (1 mL). The suspension was diluted with benzene (20−50 mL) and water (10 mL) and the

(70) O'Connell, J. F.; Parquette, J.; Yelle, W. E.; Wang, W.; Rapoport, H. *Synthesis* **1988**, 767−771.

mixture stirred for 10 min. After further washing with water (20 mL), the organic phase was separated and dried (Na_2SO_4) and the solvent removed under reduced pressure to afford the Fe(II) hemes in 80−95% yield.

Data for Fe[NHPr]. MS (ES): *m*/*e* 1466.6 $[MH]^+$, calcd for $[MH]^+$ 1466.4. UV/vis (CH_2Cl_2): λ_{max} ($10^{-3}\epsilon$, $M^{-1}\cdot cm^{-1}$) 428 (208), 534 (16). NMR assignments are given in the Supporting Information.

Data for Fe[NMe]. MS (ES): *m*/*e* 1381.3 $[MH]^+$, calcd for $[MH]^+$ 1381.4. UV/vis (CH_2Cl_2): λ_{max} ($10^{-3}\epsilon$, $M^{-1}\cdot cm^{-1}$) 426 (196), 534 (20), 564(3.5).

Data for Fe[NMePr]. MS (ES): *m*/*e* 1507.5 $[MH]^+$, calcd for $[MH]^+$ 1507.5. UV/vis (C_6H_6): λ_{max} ($10^{-3}\epsilon$, $M^{-1}\cdot cm^{-1}$) 438 (151), 536 (16). NMR assignments are given in the Supporting Information.

Synthesis of Zinc Porphyrins. To a solution of the free base porphyrin (∼100 μmol) in methanol (20 mL) was added $Zn(OAc)_2$ (2.5 equiv) and the solution stirred overnight. The mixture was diluted with water (40 mL) containing Na_2EDTA. The suspension was centrifuged and the solvent removed. The purple solid was redissolved in a minimum volume of methanol, reprecipitated with water, and recentrifuged. The solid was dried under high vacuum, redissolved in 1−5% methanol/benzene, frozen, and pumped under high vacuum overnight to provide the zinc porphyrins in 85−90% yield.

Data for Zn[NMe]. MS (ES): *m*/*e* 1392.4 $[MH]^+$, calcd for $[MH]^+$ 1392.4. UV/vis (CH_2Cl_2): λ_{max} ($10^{-3}\epsilon$, $M^{-1}\cdot cm^{-1}$) 434 (60), 564 (21), 602 (6.4). NMR assignments are given in the Supporting Information.

Data for Zn[NMePr]. MS (ES): *m*/*e* 1517.5 $[MH]^+$, calcd for $[MH]^+$ 1517.5. UV/vis (CH_2Cl_2): λ_{max} ($10^{-3}\epsilon$, $M^{-1}\cdot cm^{-1}$) 434 (63), 566 (19), 606 (6.0). NMR assignments are given in the Supporting Information.

Metalation of Imidazole Pickets with Cu(I). To M[α_3ImβF$_3$T] (5 μmol) in THF (1 mL) was added $Cu(MeCN)_4PF_6$ (5 μmol, from a standard solution of 10−15 mg of Cu(I) in 100−150 μL of acetonitrile) and the solution evaporated to dryness after 10 min. The ratio [α_3ImβF$_3$T]:Cu was checked by integration of the ^{19}F signal for the CF_3 tail of the porphyrin to the PF_6^- counterion.

Data for Fe/Cu[NMe]·PF$_6$. MS (ES): *m*/*e* 1443.4 $[M - PF_6]^+$, calcd for $[M - PF_6]^+$ 1443.3. UV/vis (CH_2Cl_2): λ_{max} ($10^{-3}\epsilon$, $M^{-1}\cdot cm^{-1}$) 426 (175), 538 (11). NMR assignments are given in the Supporting Information.

Data for Fe/Cu[NMePr]·PF$_6$. MS (ES): *m*/*e* 1569.8 $[M - PF_6]^+$, calcd for $[M - PF_6]^+$ 1569.5. UV/vis (C_6H_6): λ_{max} ($10^{-3}\epsilon$, $M^{-1}\cdot cm^{-1}$) 424 (175), 538 (11). NMR assignments are given in the Supporting Information.

Data for Zn/Cu[NMe]. MS (ES): *m*/*e* 1453.3 $[M - PF_6]^+$, calcd for $[M - PF_6]^+$ 1453.3. UV/vis (CH_2Cl_2): λ_{max} ($10^{-3}\epsilon$, $M^{-1}\cdot cm^{-1}$) 430 (65), 560 (22), 600 (5.6). NMR assignments are given in the Supporting Information.

Data for Zn/Cu[NMePr]. MS (ES): *m*/*e* 1579.5 $[M - PF_6]^+$, calcd for $[M - PF_6]^+$ 1579.4. UV/vis (CH_2Cl_2): λ_{max} ($10^{-3}\epsilon$, $M^{-1}\cdot cm^{-1}$) 430 (64), 564 (22), 602 (4.8). NMR assignments are given in the Supporting Information.

Metalation of Imidazole Pickets with Cu(II). To Zn[NMe] (5 μmol) in acetonitrile (5 mL) was added 1 equiv of $Cu(OTf)_2$ (∼5 μL of a stock solution in MeCN). The presence of multiple species is evident by ^{1}H and ^{19}F NMR. Upon addition of 1.1 equiv of Bu_4NCl, the complex precipitates. The precipitate was filtered, washed with Et_2O, and redissolved in DMF-d_7. The complex demonstrates broadened ^{1}H NMR peaks characteristic of paramagnetic compounds. A single sharp ^{19}F peak (−63.2 ppm) corresponding to the CF_3 tail is observed with an intensity equal to that of the OTf^- counterion.

Acknowledgment. This work was supported by NIH Grant GM 017880-30 and NSF Grant CHE-9612725. A Stanford Graduate Fellowship (R.B.) is gratefully acknowledged.

Supporting Information Available: Full ^{1}H NMR spectra and peak tabulation and assignments for the compounds presented here. This material is available free of charge via the Internet at http://pubs.acs.org.

IC011191P